Monomethine cyanine probes for visualization of cellular RNA by fluorescence microscopy

Methods and Applications in Fluorescence

PAPER

Monomethine cyanine probes for visualization of cellular RNA by fluorescence microscopy

Daria Aristova[1,2], **Viktoriia Kosach**[1,6], **Svitlana Chernii**[1,2], **Yuriy Slominsky**[3], **Anatoliy Balanda**[1,2], **Valeriy Filonenko**[1], **Sergiy Yarmoluk**[1,2], **Alexandru Rotaru**[4], **Hülya Gizem Özkan**[5], **Andriy Mokhir**[5,*] and **Vladyslava Kovalska**[1,2,7]

[1] Institute of Molecular Biology and Genetics NASU, 150 Zabolotnogo St., 03143 Kyiv, Ukraine
[2] Scientific Services Company Otava Ltd, 150 Zabolotnogo St., 03143 Kyiv, Ukraine
[3] Institute of Organic Chemistry NASU, 5 Murmans'ka St., 02094 Kyiv, Ukraine
[4] 'Petru Poni' Institute of Macromolecular Chemistry, Romanian Academy, Grigore Ghica Voda Alley 41A, 700487 Iasi, Romania
[5] Organic Chemistry II, Friedrich-Alexander-University of Erlangen-Nuremberg, Nikolaus-Fiebiger-Str. 10, 91058 Erlangen, Germany
[6] Now is employed by Enamine Ltd/Bienta 78 Chervonotkatska St., 02094 Kyiv, Ukraine.
[7] Dr.hab. Vladyslava Kovalska who initiated, inspired, and supervised this work suddenly passed away on 03 December 2020.
[*] Author to whom any correspondence should be addressed.

E-mail: Andriy.Mokhir@fau.de

Keywords: fluorescence probe, ribonucleic acid, double stranded deoxyribonucleic acid, cancer cells, nucleolus

Supplementary material for this article is available online

OPEN ACCESS

RECEIVED
3 March 2021

REVISED
1 June 2021

ACCEPTED FOR PUBLICATION
1 July 2021

PUBLISHED
13 July 2021

Abstract

We have studied spectral-luminescent properties of the monomethine cyanine dyes both in their free states and in the presence of either double-stranded deoxyribonucleic acids (dsDNAs) or single-stranded ribonucleic acids (RNAs). The dyes possess low fluorescence intensity in an unbound state, which is increased up to 479 times in the presence of the nucleic acids. In the presence of RNAs, the fluorescence intensity increase was stronger than that observed in the presence of dsDNA. Next, we have performed staining of live and fixed cells by all prepared dyes. The dyes proved to be cell and nuclear membrane permeant. They are photostable and brightly stain RNA-containing organelles in both live and fixed cells. The colocalization confirmed the specific nucleoli staining with anti-Ki-67 antibodies. The RNA digestion experiment has confirmed the selectivity of the dyes toward intracellular RNA. Based on the obtained results, we can conclude that the investigated monomethine cyanine dyes are useful fluorescent probes for the visualization of intracellular RNA and RNA-containing organelles such as nucleoli by using fluorescence microscopy.

Introduction

In recent years the visualization of cellular molecules, structures, and organelles by fluorescence microscopy, including super-resolution microscopy, is becoming increasingly important for biological and medical research [1–3]. The fluorescence microscopy provides a possibility for understanding the living cell processes at the subcellular resolution including, e.g., metabolic processes [4, 5].

For tracking and quantification of intracellular metabolites, ions, proteins, nucleic acids fluorescent dyes are necessary. A number of such dyes have been reported including organic fluorophores [6–8], nanostructures, e.g., quantum dots [9], and fluorescent proteins [10]. Organic fluorescent dyes are small and exhibit favorable optical properties, such as brightness and photostability relative to fluorescent proteins. They can be specifically designed to be membrane permeable to illuminate intracellular milieu or membrane impermeable to report extracellular structures [11].

The cyanine class of organic dyes has been studied for over 150 years. Thousands of cyanine derivatives have been synthesized [12]. Due to the ability of cyanines to efficiently absorb light in the visible region, cyanines became important components of photographic films, making possible the development of vibrant color images [13]. Cyanines are commonly used as laser materials [14], photosensitizers and recording media in optical discs [15]. Recently, cyanines have found biotechnological applications [13].

Furthermore, the dyes of this type have become widely used as fluorescent labels and sensors for intracellular imaging and quantification of biomacromolecules. We have previously demonstrated the application of benzothiazole-based penthametine cyanine dyes as potential far-red fluorescent probes for protein detection [16].

Unsymmetrical cyanine dyes have been used extensively in sensing applications, particularly detecting nucleic acids [17]. This class of dyes features two different heterocycles linked by a mono- or polymethine bridge. For example, Thiazole Orange (TO) has benzothiazole and quinoline heterocycles connected by a monomethine group. Different heterocycles and bridge lengths allow tuning of the excitation and emission wavelengths of these dyes throughout the visible spectrum. Various substituents can be added to the two heterocyclic nitrogens, allowing further diversification of the dye structure [18]. So far, the following monomethine cyanine dyes have worked well: dyes of SYBR family, which are very sensitive DNA and RNA probes with sensitivity level in orders of magnitude higher than that of classical DNA stain Ethidium Bromide (EtBr). The most sensitive monomethine dye SYBR Gold enables the visualization of about 20 pg of double-stranded DNA (dsDNA) in electrophoresis gels. It is substantially more sensitive than the traditionally used EtBr [19]. TO, its analogs and derivatives are best known for their fluorogenic behavior upon binding with nucleic acids [17]. These dyes exhibit very low fluorescence quantum yields in an aqueous solution, but 10^2–10^3-fold enhancement of the quantum yield is observed upon binding to the nucleic acids. The fluorescence response has been attributed to restricted torsional motion of the dye in the excited state when intercalated into dsDNA [20]. Another example is oxazole yellow. It is a fluorescent cyanine dye that selectively binds to DNA and is used to detect apoptotic cells since this dye does typically not enter live cells. However, during apoptosis, the cytoplasmic membrane becomes slightly permeable, allowing easy entry of the dye.

The good biostability of cyanine dyes allowed long-term monitoring of cellular growth dynamics *in vitro* [21]. Besides, cyanine dyes are broadly applied as stains to visualize specific organelles [22–25]. Among cell-permeant cyanine dyes can be mentioned SYTO family dyes. The SYTO dyes are somewhat lower-affinity nucleic acid stains that passively diffuse through the membranes of most cells. These UV- or visible light–excitable dyes can be used to stain RNA and DNA in both live and dead eukaryotic cells, as well as in gram-positive and gram-negative bacteria [26].

Here we report the series of cell-permeant unsymmetrical cyanine monomethine dyes for nucleoli visualization. We have previously reported a number of dyes based on a [1, 10] phenanthroline moiety with different polymethine chain lengths as fluorescent probes for nucleic acids in the cell [27]. Previously, it was suggested that monomethine cyanine dyes could be more sensitive towards RNA than dsDNA in contrast to dyes with a longer polymethine chain. We assumed that this effect is due to stacking of the monomethine dyes between nucleobases of the single stranded RNA. As a continuation of this study, in the current work, we examined a series of novel monomethine cyanine dyes (figure 1) for their sensitivity to nucleic acids and the possibility of their use in fluorescence microscopy. The spectral-luminescent properties of cyanines were characterized in the presence of nucleic acids (NA). These dyes have shown superior spectral characteristics compared to dyes in the previous study [27]. All monomethine cyanines under study showed higher specificity for RNA, while previously studied trimethine and styrylcyanine dyes did not show such selectivity. Moreover, the studied dyes show a significantly higher fluorescent response in the presence of RNA (479 times versus 51 times compared to previously studied ones), which is also accompanied by a high quantum yield (up to 44% versus 1.5%).

Benzoxazole Sl-2598 and benzothiazole quinoline dye Sl-2000 were found to be the most sensitive to nucleic acids, especially to RNA. We have performed staining of live and fixed cells of the human breast cancer cell line MCF-7 and human dermal fibroblasts by these dyes to determine their localization in the cells with consequent visualization using fluorescence microscopy. The nucleoli staining was confirmed by colocalization analysis of reported cyanine monomethine dyes with anti-Ki-67 antibodies and treatment of the cells with RNase.

Materials and methods

Spectroscopic characterization of the monomethine cyanine dyes

Synthesis of the dyes

The synthetic scheme for representative dyes is shown in figure 2. To obtain the raw materials, we used commercially available benzothiazolethione and benzooxazolethione (1), which were reacted with methyl iodide to obtain S-methyl substituted intermediates (2) [28]. Upon further heating (2) with methyl iodide or 1-(6-Iodo-hexyl)-pyridinium iodide, the corresponding quaternized compounds (3) were obtained [29]. Quaternary salts of 4-Methyl-quinolines were prepared by boiling the corresponding 4-Methyl-quinolines with alkyl halides in dioxane [30]. Monomethine cyanines Lu-2, Sl-2598 and Sl-2000 were synthesized according to the standard procedure by boiling salts in ethanol in the presence of alkali [31]. Dye (7) was obtained by condensation of benzothiazolium salt (6) with 2,6-dimethyl-4-pyrone in acetic anhydride [32]. Monomethinecyanine L-33 was synthesized by heating (7) with methylamine in DMF [33]. Dye L-29 (Cyan 40) was synthesized as previously described in [34].

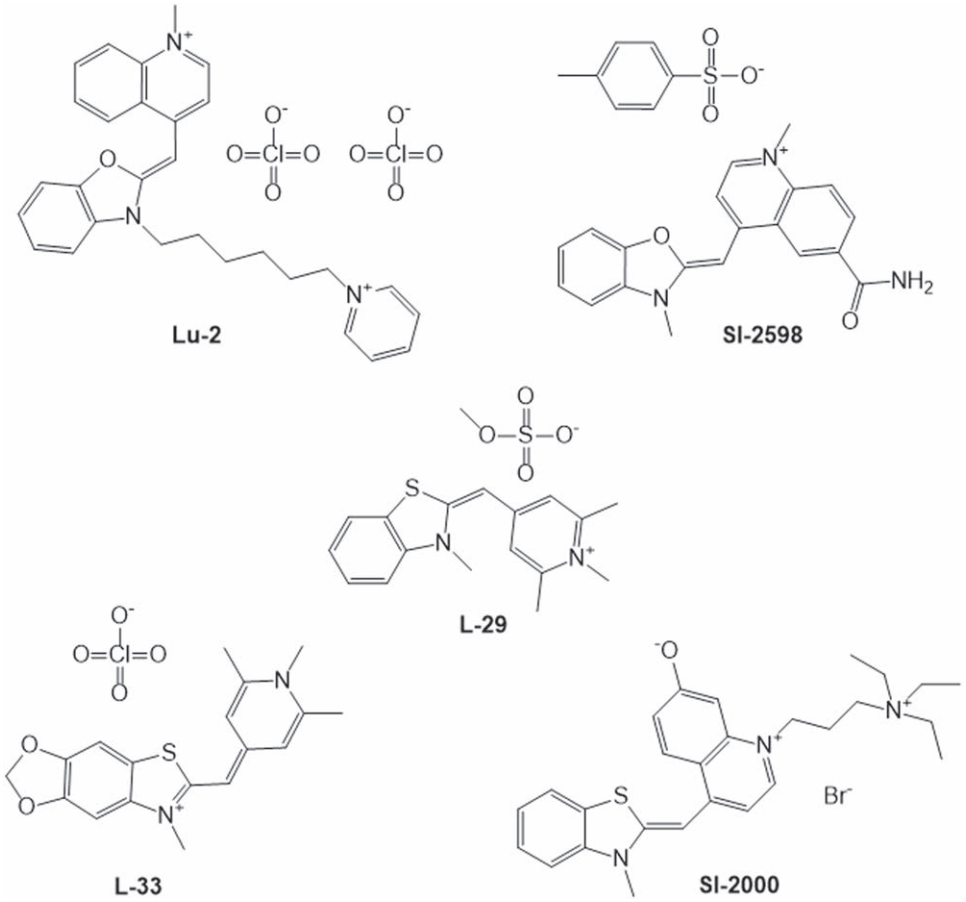

Figure 1. Chemical structures of investigated cyanine monomethine dyes.

Preparation of Lu-2

To 2-(methylthio)benzo[d]thiazole (1 g, 5.52 mmol) in a round bottom flask was added 1-(6-iodohexyl) pyridinium iodide (2 g, 6.97 mmol) and dioxane (4 ml) at room temperature. The reaction mixture was refluxed for 17 h. After removing the solvent, the crude product was used in the next step without further purification. To an ethanol solution (2 ml) of the compound obtained in the previous stage (150 mg, 0.46 mmol) and 4 (R_1, R_2 = H) (70 mg, 0.45 mmol) was added NaOH (110 μl 50% NaOH solution, 1.40 mmol) under N_2. The resulting solution was boiled while color of the reaction turned deep red. Then a sufficient amount of Na_2ClO_4 was added. After removing the solvent, the crude mixture was recrystallized twice from alcohol. Yield 36%.

Preparation of 6

To 6-Methyl-[1,3]-dioxolo[4′, 5′: 4,5]benzo[1,2-d] thiazole (1 g, 5.18 mmol) in a round bottom flask was added dimethyl sulfate (1, 3 g, 10.36 mmol) and dioxane (3 ml) at room temperature. The reaction mixture was refluxed for 14 h. After removing the solvent, the crude product was recrystallized from alcohol and washed with ether. Yield 76%.

Preparation of 7

6,7-Dimethyl-[1,3]-dioxolo[4,5-f]-[1,3]-benzothiazolium methosulfonate (0.642 g) and 2,6-dimethyl-4-pyrone (0.248 g) were dissolved in acetic anhydride (2 ml) with 1 drop of perchloric acid and refluxed for 4 h. Afterwards the reaction mixture was diluted with ethanol (4 ml). After 2 h the resulting precipitate was suction filtered and crystallized from ethanol. Yield 65%.

Preparation of L-33

To a portion of dye 7 (0.31 g, 0.75 mmol) was added DMF (4 ml) and methylamine (1 mmol) dissolved in DMF (1 ml). The mixture was refluxed for 10 min. The solvent was then evaporated under reduced pressure and ethanol (5 ml) was added, filtered and washed on the filter with ethanol and water. Yield 72%.

The structures of the new dyes were confirmed using NMR spectroscopy and HR-ESI–MS analysis. Nuclear magnetic resonance spectra were recorded on a Varian Mercury VRX-400 spectrometer using DMSO-d6 as solvent and tetramethylsilane as internal standard. Chemical shift values (δ) are quoted in ppm and coupling constants (J) in Hz. High-resolution ESI mass spectra (HR-ESI-MS) were obtained using a maXis 4G, UHR TOF mass spectrometer (Bruker Daltonik). Liquid chromatography-mass spectra (LC-MS)

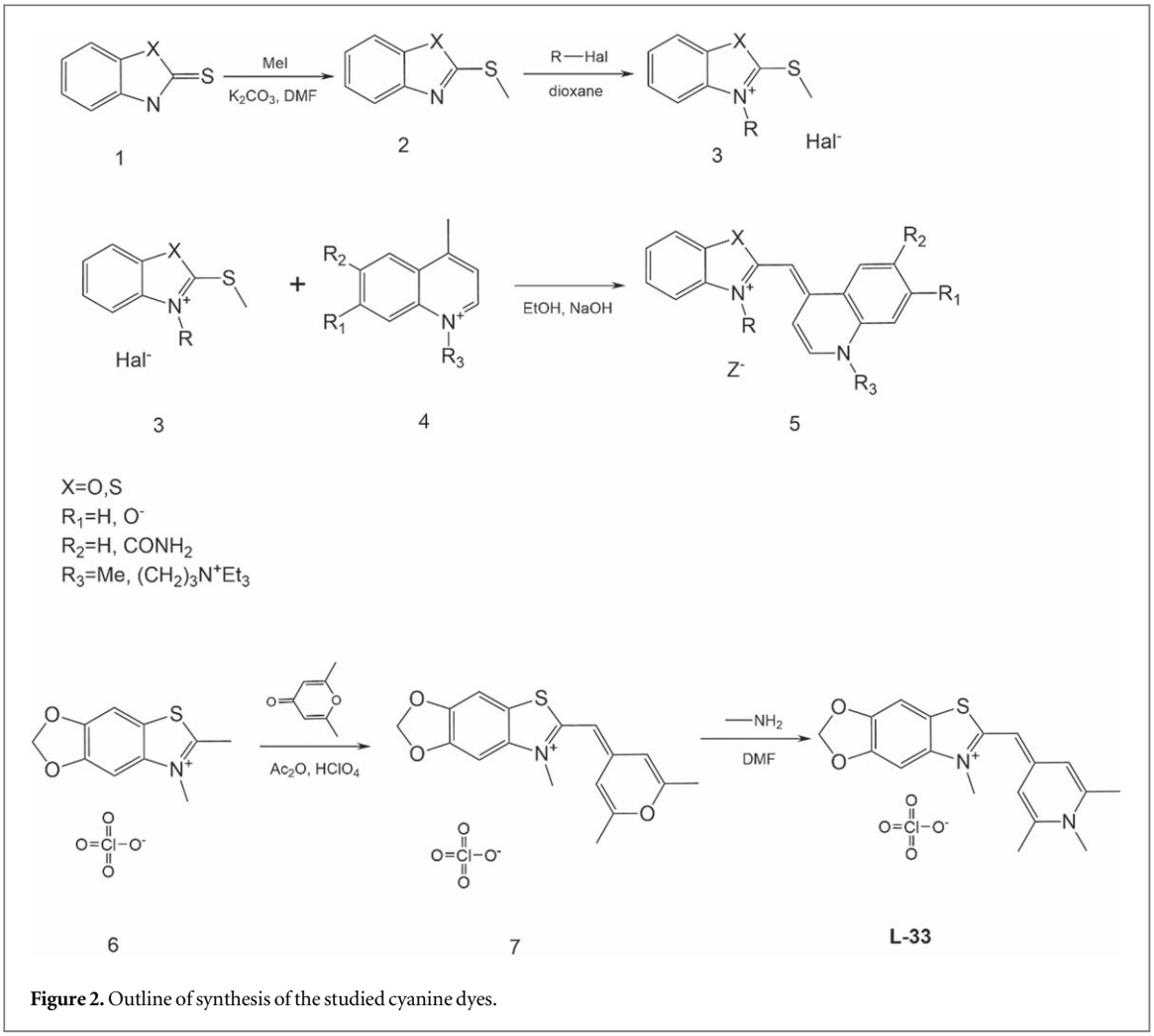

Figure 2. Outline of synthesis of the studied cyanine dyes.

analyzes were performed using the Agilent 1100 LC/MSD SL (Agilent Technologies) separations module and Mass Quad G1956B mass detector with electrospray ionization (Agilent Technologies).

6 *6,7-dimethyl-*[1,3]*dioxolo[4,5-f]*[1,3]*benzothiazol-7-ium perchlorate*:

^{1}H NMR (400MHz, DMSO-d_6): *δ*: 3.11(3H, s), 4.14(3H, s), 6.01(2H, s), 2.58(6H, s), 7.01(2H, s), 7.48 (1H, s), 7.59(1H, s). LC-MS: m/z 164 [M^+].

7 *6-[(2,6-dimethylpyran-4-ylidene)methyl]-7-methyl-*[1,3]*dioxolo[4,5-f]*[1,3]*benzothiazol-7-ium perchlorate*:

^{1}H NMR (400MHz, DMSO-d_6): *δ*: 1.97(6H, s), 3.76(3H, s), 6.14(1H, s), 6.57(2H, s), 7.03 (2H, s), 7.34 (1H, s), 7.52(1H, s). LC-MS: m/z 314 [M^+].

L-33 *7-methyl-6-[(1,2,6-trimethyl-1,4-dihydropyridin-4-yl)methyl]*[1,3]*dioxolo[4,5-f]*[1,3]*benzothiazol-7-ium perchlorate*:

Yield 72%; ^{1}H NMR (400MHz, DMSO-d_6): *δ*: 2.58 (6H, s), 3.62(3H, s), 3.73(3H, s), 5.92(1H, s), 6.11(2H, s), 7.10(2H, s), 7.35(1H, s), 7.47(1H, s). HR-ESI-MS: *m/z* 327.1167 (found, [MS^+]), 327.1162 (calculated for [$C_{18}H_{19}N_2O_2S^+$]).

SL-2000 *4-[(3-methyl-1,3-benzothiazol-3-ium-2-yl)methylene]-1-[3-(triethylammonio)propyl]-1,4-dihydroquinolin-7-olate bromide*:

Yield 41%; ^{1}H NMR (400MHz, DMSO-d_6): *δ*: 1.18 (9H, t, J = 7.0 Hz), 2.13(2H, m), 3.20–3.35 (8H + H2O, m), 3.84(3H, s), 4.40(2H, d, J = 7.1Hz), 6.64(1H, s), 6.90(1H, m), 6.97(1H, m), 7.13(1H, d, J = 7.0Hz), 7.29(1H, t, J = 7.5Hz), 7.50(1H, t, J = 7.7Hz), 7.88(1H, d, J = 7.7Hz), 8.33(1H, d, J = 7.1Hz), 8.39(1H, m). HR-ESI-MS: *m/z* 448.2408 (found, [MS^+]), 448.2417 (calculated for [$C_{27}H_{34}N_3OS^+$]).

Lu-2 *2-[(1-methylquinolin-4(1H)-ylidene) methyl]-3-(6-pyridinium-1-ylhexyl)-1,3-benzoxazol-3-ium diperchlorate*:

Yield 36%; ^{1}H NMR (400MHz, DMSO-d_6): *δ*: 1.25–1.47(4H, m), 1.73–1.73(2H, m), 4.14(3H, s), 4.39 (2H, t, J = 6.2Hz), 4.54(2H, t, J = 6.2Hz), 6.26(1H, s), 7.37(1H, t, J = 7.8Hz), 7.46(1H, t, J = 7.4Hz), 7.61 (1H, d, J = 7.6Hz), 7.77(1H, t, J = 8.2Hz), 7.95(1H, d, J = 7.3Hz), 8.01(2H, m), 8.12(2H, m), 8.46(1H, d, J = 7.3Hz), 8.56(1H, t, J = 7.4Hz), 8.74(1H, d, J = 7.5Hz), 9.02(2H, m). HR-ESI-MS: *m/z* 218.6253 (found, [MS+]), 218.1189/219.1267 ([M/M+nH], calculated for [$C_{29}H_{30}N_3O$]).

SL-2598 *2-{[6-(aminocarbonyl)-1-methylquinolin-4(1H)-ylidene]methyl}-3-methyl-1,3-benzoxazol-3-ium 4-methylbenzenesulfonate*:

Yield 45%; ^{1}H NMR (400MHz, DMSO-d_6): δ: 2.26 (3H, s), 3.89(3H, s), 4.12(3H, s), 6.31(1H, s), 7.08(1H, d, J = 7.9Hz), 7.36–7.52(4H, m), 7.66(1H, d, J = 8.1Hz), 7.81(2H, m), 7.93(1H, d, J = 7.3Hz), 8.05 (1H, d, J = 8.9Hz), 8.35–8.46(3H, m), 8.93(1H, s). HR-ESI-MS: *m/z* 332.1387 (found, [MS^+]), 332.1394 (calculated for [$C_{20}H_{18}N_3O_2^+$]).

L-29 *3-methyl-2-[(1,2,6-trimethyl-4-pyridylidene) methyl]-1,3-benzothiazol-3-ium methanesulfonate*:

Yield 76%; 1H NMR (400MHz, DMSO-d6): δ: 2.63(6H, s), 3.37(3H, s), 3.68(3H, s), 3.79(3H, s), 6.04 (1H, s), 7.24(2H,s), 7.26 (1H, d d, J1 = 7.3Hz, J2 = 9.5Hz), 7.51(2H, m), 7,83(1H, d, J = 9.5Hz). HR-ESI-MS: m/z 283.1192 (found, [MS^+]), 283.1263 (calculated for [$C_{17}H_{19}N_2S^+$]).

Preparation of working solutions of dyes and nucleic acids

Stock solutions of studied dyes were prepared in DMSO at the concentration 2 mM. Working solutions of free dyes were prepared by diluting the dye stock solution in 50 mM Tris-HCl pH 7.9 buffer or methanol. Working solutions of the dyes in the presence of nucleic acids were prepared by the addition of the aliquot of the dye stock solution to the nucleic acids stock solution. The concentrations of dye working solutions have amounted to 5 μM. Stock solutions of dsDNA (salmon testes) and yeast total RNA (Sigma-Aldrich Co) were prepared by dissolving nucleic acids in 50 mM Tris-HCl buffer pH 7.9. The concentrations of dsDNA and RNA in working solutions were equal to 6×10^{-5} M bp and 1.2×10^{-4} M bases, respectively. All working solutions were prepared immediately before the experiments.

Spectroscopy

Spectroscopic measurements were performed in a standard quartz cuvette (10 × 10 mm). Fluorescence excitation and emission spectra were registered using the fluorescent spectrophotometer Cary Eclipse (Varian, Australia). Absorption spectra were registered using the spectrophotometer Genesys 20 (Thermo-Scientific, USA) and Shimadzu UV-3600 UV–vis-NIR spectrophotometer. All the spectral-luminescent characteristics of dyes were studied at 22 °C.

Quantum yield determination

The quantum yield value of the free dyes and those in the presence of dsDNA and RNA was determined using fluorescein solution in basic ethanol as the reference (quantum yield value $\varphi_{Fl} = 0.97$) [35]. Namely, solutions of Sl-2598 and Sl-2000 in the presence of nucleic acids and solution in ethanol were taken in such concentrations that their optical density values were equal at 500 nm. Thus, the concentration of the studied dyes and fluorescein was equal 1 μM and the concentration of DNA and RNA was 6×10^{-5} M bp, 1.2×10^{-4} M bases respectively. Fluorescence of all these solutions was measured by exciting at 500 nm, and the area below each spectrum (S_{dye} for dyes and S_{Fl} for fluorescein) was calculated. Subsequently, the fluorescence quantum yield φ_{dye} of Sl-2598 and Sl-2000 in the presence of nucleic acids was calculated as: $\varphi_{dye} = \varphi_{Fl} \times (S_{dye}/S_{Fl}) \times (n_{H_2O}/n_{EtOH})^2$, where n_{H2O} and n_{EtOH} are refractive indexes of water and ethanol, respectively.

Cell culture cultivation

Human breast adenocarcinoma cell line MCF-7 was obtained from Bank of Cell Lines of the R. E. Kavetsky Institute of Experimental Pathology, Oncology and Radiobiology, NASU (Ukraine). Human dermal fibroblasts (HDF) were obtained as described in [36]. Human ovarian carcinoma A2780 cell line was obtained from Sigma-Aldrich Co.

The MCF-7 and HDF cells were cultivated in DMEM culture medium (Gibco, USA) supplemented with 10% fetal bovine serum (FBS, HyClone, USA), 4 mM glutamine, 50 units ml^{-1} penicillin, 50 μg ml^{-1} streptomycin at 37 °C in the presence of 5% CO_2. For immunofluorescence analysis cells were seeded onto sterile glass coverslips in 24-well plates 48 h before the experiments at the concentration 2×10^4 cells per well.

A2780 cells were grown in RPMI-1640 medium (Sigma-Aldrich Co.) supplemented with 10% FBS, 1% penicillin- streptomycin, 1% L-lutamine, at +37 °C in the chamber filled with5% CO_2Cells were cultivated to 80%–90% confluence and detached from the flask using trypsin/EDTA solution (0.025%/ 0.01%, w/v, Sigma Aldrich, Germany) in DPBS. A2780 cells were seeded in glass-bottom fluorescence imaging dish (μ-Dish 35 mm, high, ibidi GmbH, Germany) at the concentration 80 cells μl^{-1} in 2 ml RPMI 1640 medium containing 5% FBS, 1% L-glutamine, 1% penicillin-streptomycin 24 h prior to the experiments.

Counting cell numbers was performed via Guava easyCyte^{TM} 6-2L Flow cytometer (Merck Millipore, Darmstadt, Germany).

Fluorescence and confocal laser scanning microscopy

For live-cell imaging the growth medium was removed and the cells were washed twice by pre-heated PBS, after that the cells were incubated with cyanine dyes in FluoroBrite DMEM (Gibco, USA) without FBS for 30 min at 37 °C in the presence of 5% CO_2. Then cells were rewashed with PBS and placed in FluoroBrite DMEM.

The cells were fixed in 10% neutral buffered formalin (Sigma-Aldrich, USA) for 15 min at 22 °C for microscopy of fixed cells. Cell membranes were permeabilized with 0.2% Triton X-100 in PBS for 10 min at 22 °C. After that, cells were incubated with 10 mM cupric sulphate and 50 mM ammonium acetate, pH 5.0 for 30 min at 22 °C to reduce autofluorescence. Next cyanine dyes in PBS were added to the samples for 30 min at 22 °C in the dark. Among all incubations, the cells were washed three times with PBS. At the end,

the samples were embedded into Mowiol 4–88 mounting medium (Sigma-Aldrich, USA) containing 2,5% DABCO (Sigma-Aldrich, USA).

For colocalization analysis, cells were fixed and permeabilized as described. After the autofluorescence reduction the samples were incubated with 1% BSA for 1 h at 22 °C. Afterwords mouse monoclonal antibodies against Ki-67 protein (1:200) were added to the cells and incubated overnight at 4 °C. The anti-Ki-67 antibodies were generated and evaluated earlier [37]. The TRITC-AffiniPure Goat Anti-Mouse IgG (H + L) secondary antibody (Jackson ImmunoResearch Labs, USA) was applied at 1:400 for 40 min at 37 °C in humidified chamber. The mix of the cyanine dyes and Hoechst 33342 (Invitrogen, ThermoFisher Scientific, USA) in PBS were added to the samples for 30 min at 22 °C in the dark. After each incubation, the cells were washed with PBS. Samples were embedded into Mowiol 4–88 (Sigma-Aldrich, USA) containing 2,5% DABCO (Sigma-Aldrich, USA).

Microscopy image acquisition was performed using either Leica DM 1000 epifluorescent microscope with excitation filter 355–425 nm for Hoechst 33342, and 450–490 nm for dyes or Zeiss LSM 510 META laser scanning confocal microscope (Carl Zeiss Microscopy GmbH, Germany), using excitation at 405 nm for Hoechst 33342, excitation at 488 nm for studied dyes, and excitation at 543 nm for anti-Ki-67 antibodies. Obtained images were analyzed using free software Fiji/ImageJ v1.52b [38].

RNA digestion experiment

The growth medium was removed, and the cells were washed twice by pre-heated PBS. For fixation, the cells were covered with 1 ml of cold MeOH and incubated for 15 min at −20 °C. Afterward, the cells were washed twice with PBS and 2 ml RNase A (Sigma-Aldrich Co) solution (0.1 mg ml^{-1} RNase A in PBS) was added and incubated for 3 h at 37 °C. As a negative probe, the cells were treated with 2 ml of PBS for 3 h at 37 °C. After incubation, the medium was removed, and the cells were washed with PBS twice. 2 ml of the solution of the dyes in PBS was added and incubated for 30 min at 22 °C. After that, cells were washed with PBS and microscopy images were taken. The fluorescence microscopy images were taken with a Zeiss Axio Vert. A1 with filter set: ex 450–490 nm, em 500–550 nm (green) for the detection of dyes and ex 335–383/em 420–470 nm (blue) for the detection of Hoechst 33342.

Results

Photophysical properties of the synthesized monomethine cyanine dyes

We have acquired VIS spectra of the studied dyes in methanol and in aqueous buffer 50 mM Tris-HCl, pH 7.9 (table 1, figures 3(a), (b)). The absorption maxima of the monomethine cyanines in methanol are located in the range of 438–492 nm (figure 3(a)), the molar extinction values are in the range (4.5–8.0) × 10^4 M^{-1} cm^{-1}.

Table 1. Molar extinction coefficient at λ_{max}. of the dyes (5 μM) in methanol and 50 mM Tris-HCl buffer (pH 7,9).

Dye	Tris-HCl, pH 7.9 ε, 10^4 M^{-1} cm^{-1}	MeOH
Sl-2000	4.0	4.5
L-33	3.9	4.6
Sl-2598	6.1	6.9
Lu-2	6.8	7.9
L-29	8.1	8.0

ε—molar extinction coefficient at λ_{max}.

The absorption maxima of the monomethine cyanines in the aqueous buffer are located in the range of 435–490 nm (figure 3(b)) with the molar extinction values between (3.9–8.1) × 10^4 M^{-1} cm^{-1}. These values are lower than in methanol, except of dye L-29. The shape of spectra almost has not changed with shoulders at a shorter wavelength for dyes Lu-2 and Sl-2598. The minor differences between the spectra in methanol and the buffer solution indicate that these dyes exist in both media as monomers. Spectral-luminescent properties of the series of monomethine cyanine dyes in the buffer solution and the presence of nucleic acids are presented in table 2.

The studied dyes possess low fluorescence intensity in the aqueous buffer (figure 4). Fluorescence maxima of these dyes in the free state are located in the range 515–608 nm and the addition of nucleic acids leads to the hypsochromic shift of the emission maximum (up to 82 nm for dye Sl-2000) in the range 506–529 nm. On the contrary, the bathochromic shift (467–505 nm) for excitation maxima is observed. As a result, a decrease in the Stokes shift was observed.

The binding to nucleic acids results in a significant increase in fluorescence intensity of the studied dyes. We have observed that benzoxazole quinoline dye Sl-2598 and benzothiazole quinoline dye Sl-2000 exhibit the strongest nucleic acid-induced fluorescence enhancement. The fluorescence intensity of these dyes increases in the presence of RNA by 479 and 402 times, respectively (table 2, figure 4, Suppl. material SM1 (available online at stacks.iop.org/MAF/9/045002/mmedia)). We have estimated the quantum yield value for dye Sl-2598 in the presence of dsDNA and RNA. It was found to be equal to 32% and 44%, respectively.

Other studied dyes are also found to be sensitive to nucleic acids; they demonstrate an increase of emission intensity up to 306 times in the presence of RNA and by 50–200 times in the presence of dsDNA. As expected, in the presence of BSA, an insignificant increase of fluorescence intensity was observed (2–5 t., Suppl. material SM2). These data indicate that studied monomethine cyanines displayed strong selectivity to

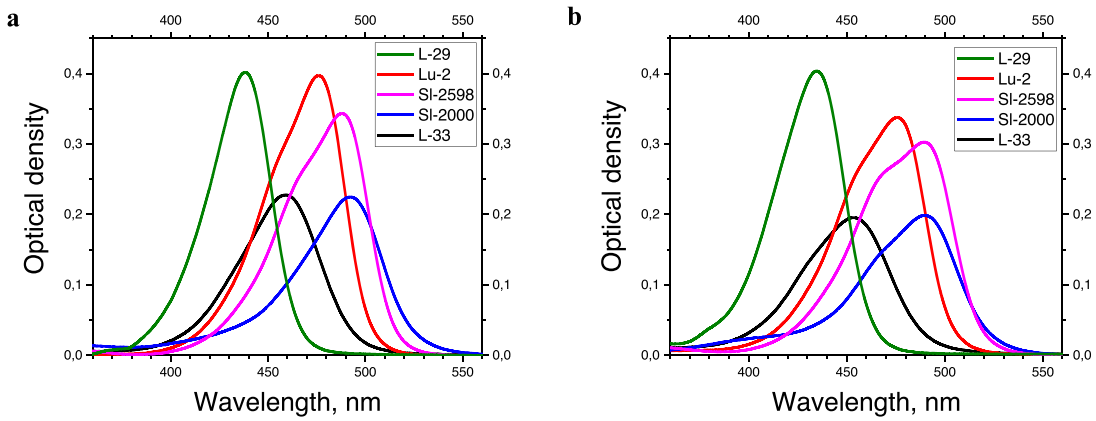

Figure 3. The absorption spectra of the studied cyanine dyes in MeOH (a) and in 50 mM Tris-HCl (pH 7.9) (b). Dye concentration 5 μM.

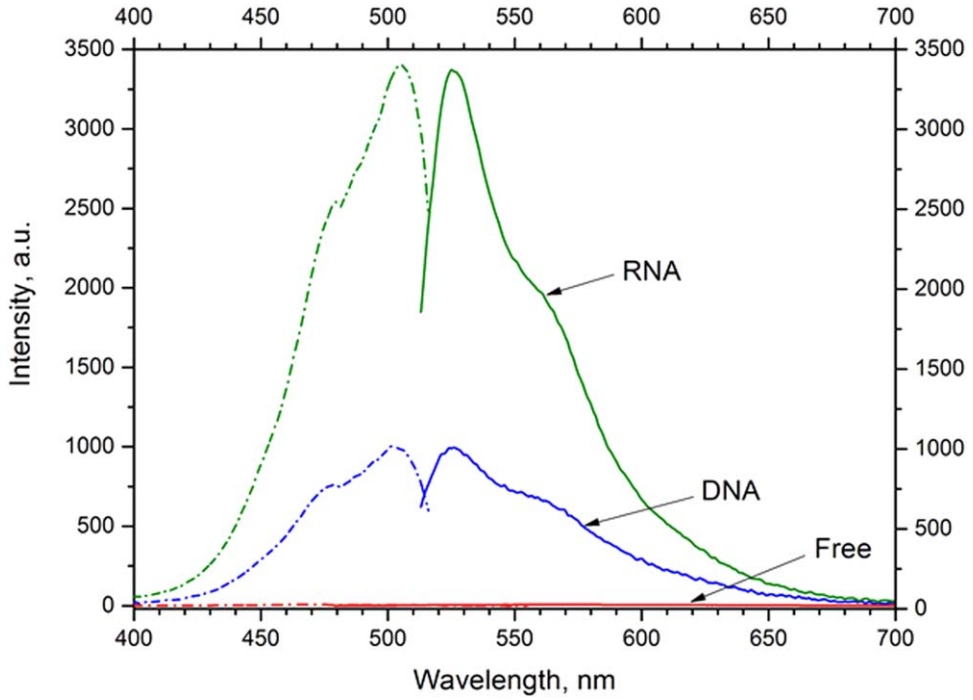

Figure 4. Fluorescence emission (right) and excitation (left) spectra of Sl-2598 in unbound state and in the presence of dsDNA and RNA. Dye concentration 5 μM.

Table 2. Spectral-luminescent properties of cyanine dyes in free state and in the presence of nucleic acids.

	Free			dsDNA			RNA		
Dye	$\lambda_{ex.}$	$\lambda_{em.}$	I, a.u.	$\lambda_{ex.}$	$\lambda_{em.}$	$I_{Free/dsDNA}$	$\lambda_{ex.}$	$\lambda_{em.}$	$I_{Free/RNA}$
Sl-2000	465	608	5	505	526	207 t.	506	529	402 t.
L-33	462	524	14	467	506	50 t.	468	506	180 t.
Sl-2598	468	564	7	502	526	141 t.	504	526	479 t.
Lu-2	480	515	10	488	511	113 t.	489	511	306 t.
L-29	434	469	8	453	475	24 t.	451	476	128 t.

$\lambda_{ex.}$ ($\lambda_{em.}$)—maximum wavelength of fluorescence excitation (emission) spectrum; I—emission intensity of dye in free state (in a.u.—arbitrary units); $I_{Free/dsDNA}$ ($I_{Free/RNA}$)—incresment of the dyes fluorescent intensity in the presence of dsDNA (RNA) (in t.—number of times).

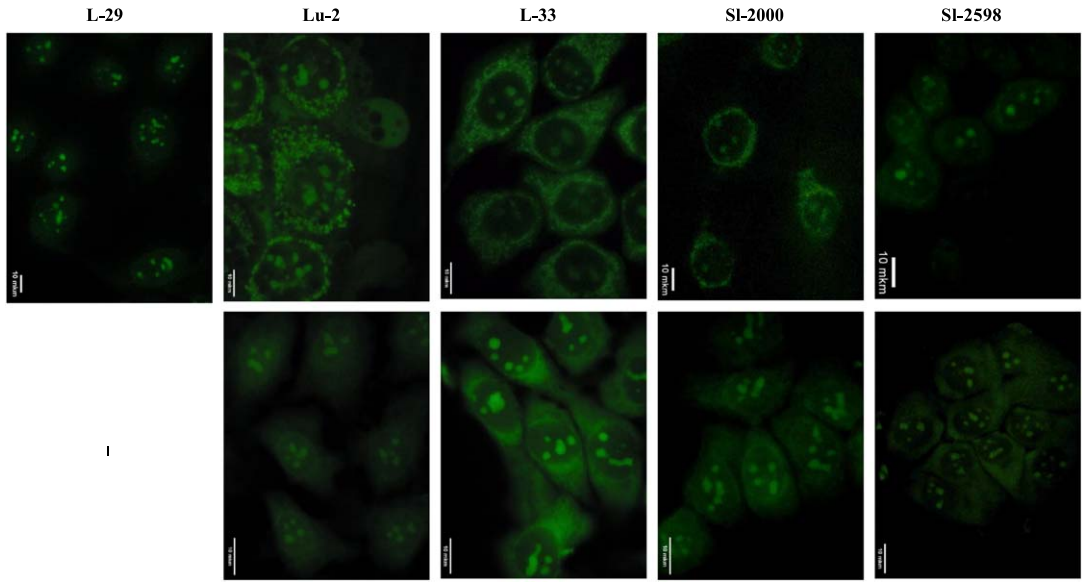

Figure 5. Fluorescence image of live cell MCF-7 stained with the dye L-29 (0.1 μM), Lu-2 (0.1 μM), L-33 (0.1 μM), Sl-2000 (0.1 μM), and Sl-2598 (C = 10 μM). Scale bars–10 μm.

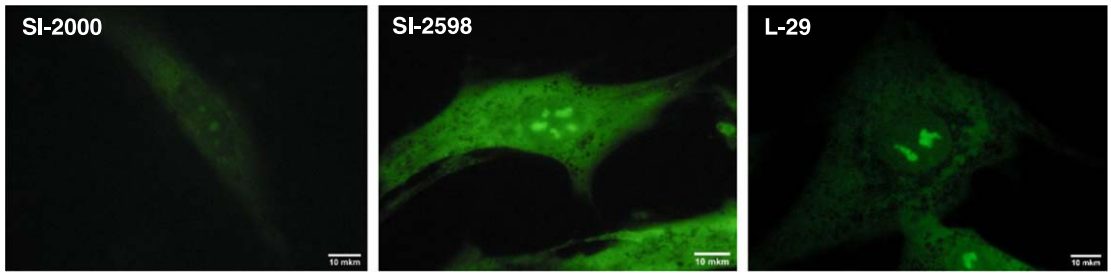

Figure 6. Fluorescence image of live fibroblasts staining by Sl-2000, Sl-2598 and L-29. The cells were incubated with 20 μM Sl-2000, 5 μM Sl-2598 and 1 μM L-29 for 30 min. Scale bars–10 μm.

nucleic acids while being entirely insensitive to globular protein.

Moreover, all dyes give a stronger response in the RNA presence compared to dsDNA. Obtained results are consistent with previously described dyes based on a [1, 10] phenanthroline moiety with shorter length of polymethine chain [27]. Thus, the studied monomethine cyanine dyes can be considered as specific probes for detecting RNA due to their high fluorescent response in the presence of this type of nucleic acid.

The fluorescence microscopy study

We first examined the applicability of the studied monomethine cyanine dyes in staining live and fixed MCF-7 cells. This cell line is a well characterized, widely used breast cancer model with adherent and nicely spread cells suitable for imaging of sub-cellular architecture [39]. The cells were incubated with different dye concentrations −10 μM, 1 μM, 0.1 μM with the aim to determine the sensitivity of detection of the dyes within the cells. Irradiation with 450–490 nm wavelength was used to excite the fluorescence of the cyanine dyes. Fluorescence microscopy images of the stained live and fixed cells are presented in figure 5. It was shown that studied dyes can be detected with different sensitivity. Optimal results were obtained at the following concentrations: 10μM for Sl-2598 dye, and 0.1μM for L-33, L-29, Sl-2000 and Lu-2 dyes for live cells, and 1 μM for all dyes for staining of fixed cells, except for dye L-29, which does not stain fixed cells.

We have found that all dyes proved to be membrane-permeant and stain the sub-cellular components in live cells. However, it should be mentioned that benzoxazole dye Lu-2 with a positive charge in the N-alkyl tail group caused damage to cell membranes in live cells. Thus, this dye is more suitable for the fixed cells imaging.

All studied dyes besides L-29 have partially accumulated in the cytoplasm and gave a weak fluorescent green background. We believe this signal belongs to the weak staining of live cell RNA in the cytoplasm. However, the dye L-33 quite distinctly stained some branched granules in the cytoplasm. We suppose that it probably could be rough endoplasmic reticulum or mitochondria.

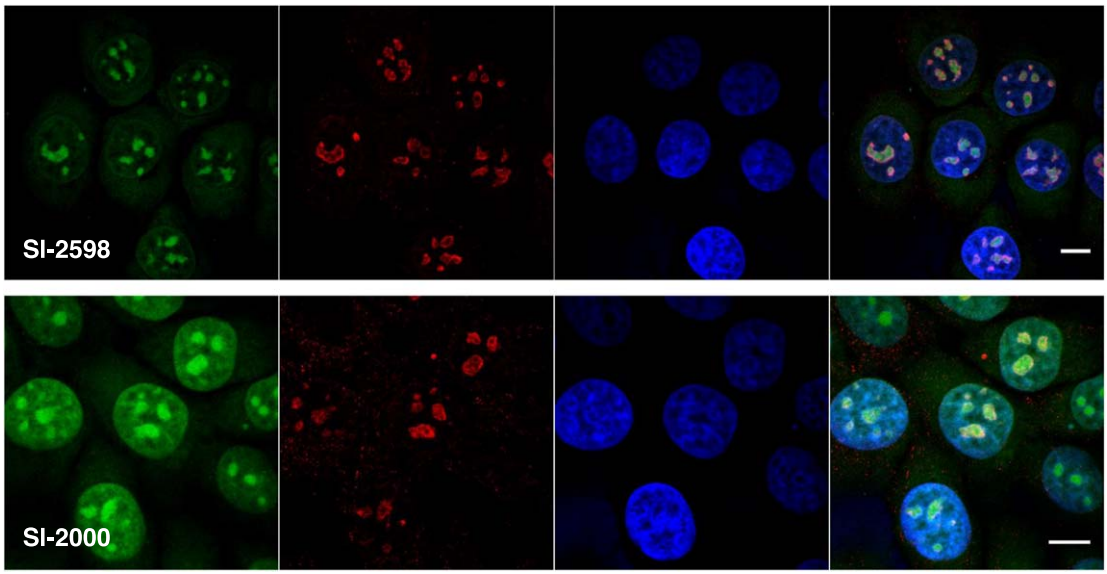

Figure 7. CLSM images of colocalization of Sl-2598 and Sl-2000 dyes with antibodies against Ki-67 protein in MCF-7 cells. (green—studied dyes, red—antibodies against Ki-67 protein, blue—Hoechst, $C_{dye} = 1\ \mu M$, $C_{Ki\text{-}67} = 10\ \mu M$.) Scale bars–10 μm.

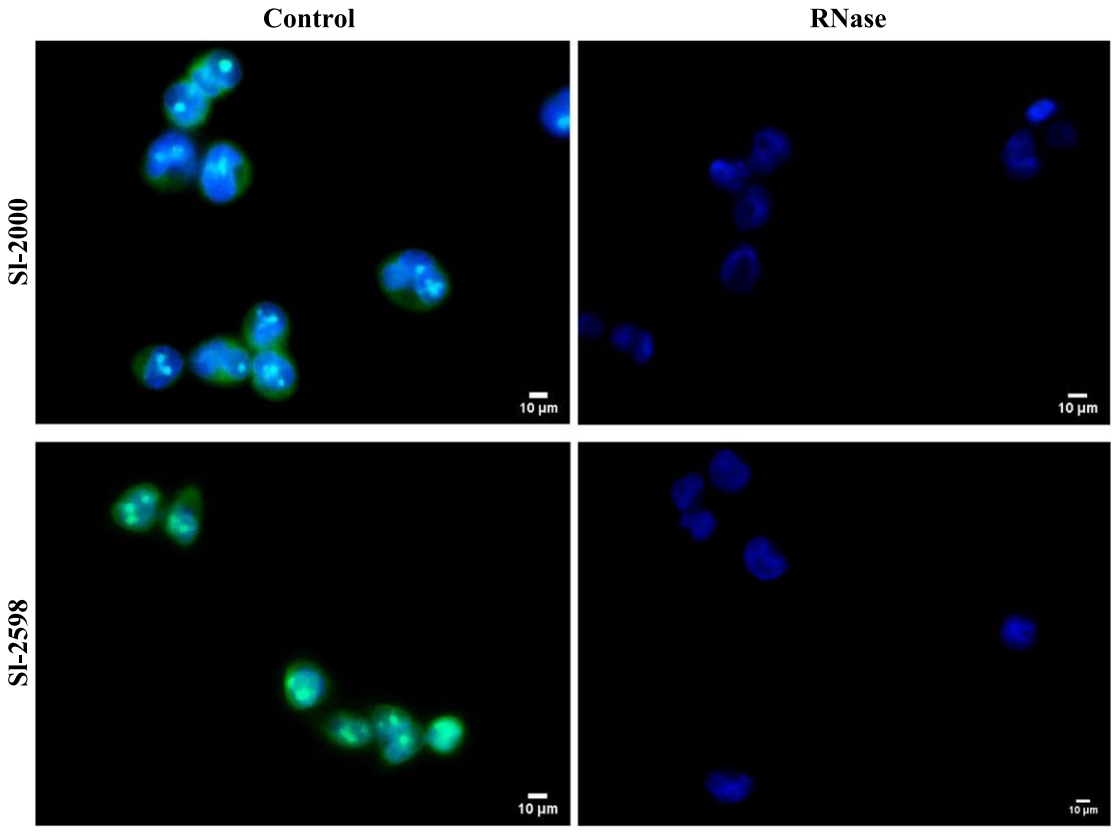

Figure 8. RNase A-untreated (left) and treated fixed A2780 cells (right) stained by the dye Sl-2000 and Sl-2598 (green—studied dyes, blue—Hoechst 33342). Scale bars–10 μm.

Moreover, all studied dyes penetrated the nuclear membrane and stained large structures within the nucleus, most probably nucleoli. In the previous study [40] L-29 was taken at the concentration of 10 μM, and besides staining of structures within the nucleus, bright staining of cytoplasm was observed. In the current experiment, we have decreased concentrations down to 0.1 μM for this dye, which permitted a strong decrease in fluorescence within the cytoplasm but keeping the nucleoli brightly stained (figure 5).

In fixed cells, the studied dyes possessed similar behavior with a slightly stronger fluorescence in the

cytoplasm. Dye L-29 did not stain fixed cells at studied concentrations.

As mentioned above, benzoxazole dye Lu-2 caused damage to cell membranes in live cells. Though L-33 showed high sensitivity, it stained several cell structures and therefore it is not an organelle-specific probe. Thus, we have chosen Sl-2598, Sl-2000, and L-29 as the most promising dyes for the organelle-specific cell staining for further research.

Staining of human dermal fibroblasts by the dyes Sl-2000, Sl-2598 and L-29

Membrane potential (Vm) in cancer cells is different from that in normal cells. In particular, it has been shown that Vm is depolarized in many types of cancer cells [41, 42]. Furthermore, cell surface of cancer cells is negatively-charged, whereas that of normal cells is either charge-neutral or slightly positive [43]. Since all studied here dyes are charged, we assumed that they could be able to differentiate between cancer and normal cells. We found that Sl-2598, L-29 and Sl-2000 are membrane-permeant and stain cytoplasm and nucleoli in normal cells (dermal fibroblasts) as well as in cancer cells (MCF-7). However, the optimal concentrations of the dyes L-29 and Sl-2000 suitable for staining normal human dermal fibroblasts was higher than that used for MCF-7 cells: 1 (L-29)and 20 μM (SI-2000) versus 0.1 μM respectively .

In contrast, dye Sl-2598 stained normal cells at the concentration of 5 μM, which is comparable to that found optimal for the cancer cells: 10 μM (figure 6). These data indicate that dyes L-29 and Sl-2000 can used to selectively stain cancer cells in the presence of normal cells at the concentration of 0.1 μM that could potentially be used for cancer diagnostics and biological research,

Photobleaching is an important parameter characterizing the properties of the investigated dyes. Unlike quenching, which can be reversible, photobleaching is generally irreversible [44]. We observed that under direct irradiation of the dermal fibroblast cells stained with benzoxazole quinoline dye Sl-2598 with light at 450–490 nm (OSRAM mercury lamp 50W luminous intensity 230 cd, microscope Leica DM 1000 epifluorescent microscope) the fluorescent staining of nucleoli remained stable for 7 min. The stability of dyes Sl-2000 and L-29 was found to be ~5 times lower (Suppl. material SM3, SM4). We suggest that the difference in the photostability of the dyes may be due to the difference in the binding efficiency to the RNA. Dye Sl-2598 has the highest increase in fluorescence intensity in the presence of RNA with an impressive quantum yield of 44% and, thus, the highest stability to photobleaching.

Confirmation of staining of intracellular RNA by dyes Sl-2000 and Sl-2598

The studied dyes stained bright large puncta in the nuclei of cancer and normal human cells. We assume that it may be nucleoli. We used antibodies against Ki-67 protein for a colocalization analysis using confocal laser scanning microscopy (CLSM) to investigate this possibility. The Ki-67 antigen is detected in proliferating cells in all phases of the cell division cycle. During most of the interphase, namely at S and G2 stages pKi-67 is present within nucleoli [45]. In figure 7 we can see the colocalization of the studied dyes and Ki-67 that confirms that dyes Sl-2000 and Sl-2598 stain nucleoli. Since the L-29 doesn't stain fixed cells we could not perform such an experiment for this dye.

It is known that nucleoli have three components including (1) fibrillar centers (FCs) surrounded by (2) dense fibrillar components (DFC's), which are embedded within (3) granular components (GC's). rRNA in nucleoli are mainly located at the DFC and GC components [46–48]. Overall, our data suggest that the dyes bind intracellular RNA including nucleoli and cytoplasm-located RNA. To further confirm this point, we performed the control experiment, in which the RNA in fixed cells was digested by using ribonuclease (RNase A). Then the cells were stained with dye Sl-2000 and Sl-2598. We used A2780 cells for this experiment. The fluorescence images of RNase A-untreated and treated fixed A2780 cells are shown in figure 8. It is apparent that nucleoli- and cytoplasm-located signal of the dyes is fully absent in RNase A-treated cells. These results unambiguously confirm that the studied dyes Sl-2000 and Sl-2598 bind specifically to RNA in nucleoli and also in cytoplasm that correlates with the previously described spectral-luminescent measurements indicating the higher fluorescent response of the dyes to RNA than to dsDNA.

Conclusion

We have studied a series of monomethine cyanines for cell RNA-specific staining of live and fixed cells. We have observed that all dyes exhibit the strong fluorescent 'light-up' response in the presence of nucleic acids including RNA and double stranded DNA. In contrast, they gave the low response in the presence of proteins, particularly serum albumin. The free dyes possess emission at 515–608 nm when excited at 462–480 nm. All dyes were found to be more responsive to RNA than to dsDNA. The most efficient benzothiazole quinoline dye Sl-2000 and benzoxazole quinoline dye Sl-2598 demonstrate the increase of the fluorescence intensity up to 400 and 480 times in the presence of RNA, respectively. By using fluorescence microscopy we have shown that all dyes are sensitive to intracellular RNA including RNA-rich organelles nucleoli in the nucleus and cytoplasmic RNA. Under the optimized conditions dyes Sl-2000, Sl-2598, and L-29 can be used as nucleoli-specific fluorescent probes. The colocalization with antibodies to Ki-67 protein as well as experiments with RNase A-treated fixed cells unambiguously confirmed that dyes Sl-2000 and Sl-2598 stain RNA in nucleoli. Finally, we observed that

under the optimized conditions the dyes can be used to selectively stain cancer cells in the presence of normal cells.

Acknowledgments

The project NoBiasFluors leading to these results has received funding from the European Union's Horizon 2020 research and innovation programme under the Marie Skłodowska-Curie grant agreement No. 872331.

The authors have declared that no conflicting interests exist.

Data availability statement

All data that support the findings of this study are included within the article (and any supplementary files).

ORCID iDs

Viktoriia Kosach https://orcid.org/0000-0002-8214-9604
Svitlana Chernii https://orcid.org/0000-0003-2034-8429
Andriy Mokhir https://orcid.org/0000-0002-9079-5569
Vladyslava Kovalska https://orcid.org/0000-0001-8305-9398

References

[1] Sanderson M J, Smith I, Parker I and Bootman M D 2014 *Cold Spring Harbor Protocols* **2014** 1024–65
[2] Möckl L and Moerner W E 2020 *J. Am. Chem. Soc.* **142** 17828–44
[3] Stockhammer A and Bottanelli F 2021 *J. Phys. D: Appl. Phys.* **54** 033001
[4] Schneider A F L and Hackenberger C P R 2017 *Curr. Opin Biotechnol.* **48** 61–8
[5] Uchinomiya S, Matsunaga N, Kamoda K, Kawagoe R, Tsuruta A, Ohdo S and Ojida A 2020 *Chem. Commun.* **56** 3023–6
[6] Johnson I 1998 *Histochem J.* **30** 123–40
[7] Zhu H, Fan J, Du J and Peng X 2016 *Acc. Chem. Res.* **49** 2115–26
[8] Choi N E, Lee J Y, Park E C, Lee J H and Lee J 2021 *Molecules* **26** 217
[9] Kargozar S, Hoseini S J, Milan P B, Hooshmand S, Kim H-W and Mozafari M 2020 *Biotechnol. J.* **15** 2000117
[10] Rodriguez E A, Campbell R E, Lin J Y, Lin M Z, Miyawaki A, Palmer A E, Shu X, Zhang J and Tsien R Y 2017 *Trends Biochem Sci.* **42** 111–29
[11] Specht E A, Braselmann E and Palmer A E 2017 *Annu. Rev. Physiol.* **79** 93–117
[12] Mishra A, Behera R K, Behera P K, Mishra B K and Behera G B 2000 *Chem. Rev.* **100** 1973–2012
[13] Armitage B A 2008 *Cyanine Dye–Nucleic Acid Interactions Heterocyclic Polymethine Dyes (Topics in Heterocyclic Chemistry* ed L Strekowski 14 (Berlin, Heidelberg: Springer) pp 11–29
[14] Reisfeld R, Weiss A, Saraidarov T, Yariv E and Ishchenko A 2004 *Polymers Adv. Technol.* **15** 291–301
[15] Henary M, Paranjpe S and Owens E 2013 *Heterocyclic Communications.* **19** 1–11
[16] Aristova D, Volynets G, Chernii S, Losytskyy M, Balanda A, Slominskii Y, Mokhir A, Yarmoluk S and Kovalska V 2020 *R. Soc. Open Sci.* **7** 200453
[17] Lee L G, Chen C H and Chiu L A 1986 *Cytometry.* **7** 508–17
[18] Gloria L S, Volkan E, Yaron D and Armitage B A 2007 *J. Am Chem. Soc.* **129** 5710–718
[19] Tuma R S, Beaudet M P, Jin X, Jones L J, Cheung C-Y, Yue S and Singer V L 1999 *Anal Biochem.* **268** 278–88
[20] Netzel T L, Nafisi K, Zhao M, Lenhard J R and Johnson I 1995 *J. Phys. Chem.* **99** 17936–47
[21] Gaur P, Kumar A, Dalal R, Bhattacharyya S and Ghosh S 2017 *Chem. Commun.* **53** 2571–4
[22] Guo L, Chan M S, Xu D, Tam D Y, Bolze F, Lo P K and Wong M S 2015 *ACS Chem Biol.* **10** 1171–5
[23] Abeywickrama C S, Wijesinghe K J, Stahelin R V and Pang Y 2017 *Chem. Commun.* **53** 5886–9
[24] Liu Y, Zhou J, Wang L, Hu X, Liu X, Liu M, Cao Z, Shangguan D and Tan W 2016 *J. Am. Chem. Soc.* **138** 12368–74
[25] Zhang S, Fan J, Li Z, Hao N, Cao J, Wu T, Wang J and Peng X 2014 *J. Mater. Chem. B.* **2** 2688–93
[26] Johnson I D and Spence M T Z 2010 *The Molecular Probes Handbook: A Guide To Fluorescent Probes And Labeling Technologies* 11th edn (Carlsbad, CA, USA: Life Technologies) 307–14 0982927916
[27] Kovalska V, Kuperman M, Varzatskii O, Kryvorotenko D, Kinski E, Schikora M, Janko C, Alexio C, Yarmoluk S and Mokhir A 2017 *Methods Appl. Fluoresc.* **5** 045002
[28] Bethge L, Jarikote D V and Seitz O 2008 *Bioorganic & Medicinal Chemistry* **16** 114–25
[29] Lai H-P, Gao R-C, Huang C-L, Chen I-C and Tan K-T 2015 *Chem. Commun. (Camb)* **51** 16197–200
[30] Tokar V P *et al* 2006 *J Fluoresc* **16** 783–91
[31] Hamer F M 1964 *The Cyanine Dyes and Related Compounds* ed J Willey (New York, NY: Wiley) p 37
[32] Yarmoluk S M, Kostenko O M, Tolmachev O I and Wolfbeis O S 2003 *US Patent No. US* 2003/0175988A1, Appl. Sep. 18
[33] Kryvorotenko D V, Kovalska V B and Yarmoluk S M 2000 *Biopolym. Cell.* **16** 145–52 (in Ukrainian)
[34] Lukashov S S, Kachkovskyy G O, Losytskyy M Y and Yarmoluk S M 2001 *Biopolym. Cell.* **17** 242–8 (in Ukrainian)
[35] Seybold P G, Gouterman M and Callis J 1969 *Photochem Photobiol.* **9** 229–42
[36] Nizheradze K A 2000 *Folia Histochem Cytobiol.* **38** 167–73 PMID: 11185721
[37] Khoruzhenko A, Kukharchuk V, Cherednyk O, Tykhonkova I, Ovcharenko G, Malanchuk O and Filonenko V 2010 *HYBRIDOMA* **29** 301–4
[38] Schindelin J *et al* 2012 *Nat Methods* **9** 676–82
[39] Comşa Ş, Cîmpean A M and Raica M *Anticancer Res.* **35** 3147–54 PMID: 26026074
[40] Ohulchanskyy T Y, Pudavar H E, Yarmoluk S M, Yashchuk V M, Bergey E J and Prasad P N 2003 *Photochem Photobiol.* **77** 138–45
[41] Binggeli R and Cameron I L 1980 *Cancer Res* **40** 1830–5 PMID: 7371014
[42] Yang M and Brackenbury W J 2013 *Front Physiol.* **4** 185
[43] Le W, Chen B, Cui Z, Liu Z and Shi D 2019 *Biophys Rep* **5** 10–8
[44] Ghiran I C 2011 *Introduction to Fluorescence Microscopy. Light Microscopy (Methods in Molecular Biology)* ed H Chiarini-Garcia and R Melo 689 (Totowa, NJ: Humana Press) pp 93–136
[45] Kill I R 1996 *J. Cell Sci.* **109** 1253–63 PMID: 8799815
[46] Sirri V, Urcuqui-Inchima S, Roussel P and Hernandez-Verdun D 2008 *Histochem Cell Biol.* **129** 13–31
[47] Cmarko D, Verschure P J, Rothblum L I, Hernandez-Verdun D, Amalric F, van Driel R and Fakan S 2000 *Histochem Cell Biol.* **113** 181–7
[48] Biggiogera M, Fakan S, Kaufmann S H, Black A, Shaper J H and Busch H 1989 *J. Histochem. Cytochem.* **37** 1371–4